EPJ manuscript No.
(will be inserted by the editor)

Droplet migration: Quantitative comparisons with experiment

Y.Y. Koh[1], Y.C. Lee[2], P.H. Gaskell[2], P.K. Jimack[3], and H.M. Thompson[2,a]

[1] INTI International University College, Negeri Sembilan, Malaysia 71800
[2] School of Mechanical Engineering, University of Leeds, Leeds, United Kingdom LS2 9JT
[3] School of Computing, University of Leeds, Leeds, United Kingdom LS2 9JT

Abstract. An important practical feature of simulating droplet migration computationally, using the lubrication approach coupled to a disjoining pressure term, is the need to specify the thickness, H^*, of a thin energetically stable wetting layer, or precursor film, over the entire substrate. The necessity that H^* be small in order to improve the accuracy of predicted droplet migration speeds, allied to the need for mesh resolution of the same order as H^* near wetting lines, increases the computational demands significantly. To date no systematic investigation of these requirements on the quantitative agreement between prediction and experimental observation has been reported. Accordingly, this paper combines highly efficient Multigrid methods for solving the associated lubrication equations with a parallel computing framework, to explore the effect of H^* and mesh resolution. The solutions generated are compared with recent experimentally determined migration speeds for droplet flows down an inclined plane.

1 Introduction

Droplet migration and wetting phenomena are ubiquitous throughout science and engineering and are crucial to several natural, engineering and manufacturing processes. A key issue in related theoretical studies is the alleviation of the stress singularity at dynamic wetting lines and for which several models have been proposed, see for example [1]. Analytical investigations apart [2], numerical solutions, based on lubrication theory coupled with a disjoining pressure term, to alleviate the stress singularity at dynamic wetting lines, have increasingly appeared, which explore droplet motion: (i) on chemically- and topographically-heterogeneous substrates [3,4]; (ii) driven by external body or Marangoni forces [5,6].

Despite the above successes, an important feature of using the disjoining pressure term, is the need to specify the thickness of a thin energetically stable wetting layer, or precursor film, H^*, over the whole of the substrate, which experimental evidence suggests lies in the broad range $1-100\,\mathrm{nm}$ [7]. To improve computational accuracy it is necessary to use small H^* values in order to achieve droplet migration speeds commensurate with experimentally observed ones [8]. This requirement increases the computational demands significantly since mesh resolution near wetting lines must be of the same order as H^* in order to avoid highly inaccurate, oscillatory or even negative film thicknesses being predicted. No systematic investigation into these effects on the quantitative agreement with experimental data has been performed to date. However, the need for such is highlighted in a recent comparison of numerical solutions [5] with the experiments of Podgorski et al [8] and Le Grand et al [9] for droplet migration down an inclined plane, see Fig 1. Although good qualitative agreement can be obtained without highly resolved

---

[a] e-mail: `h.m.thompson@leeds.ac.uk`

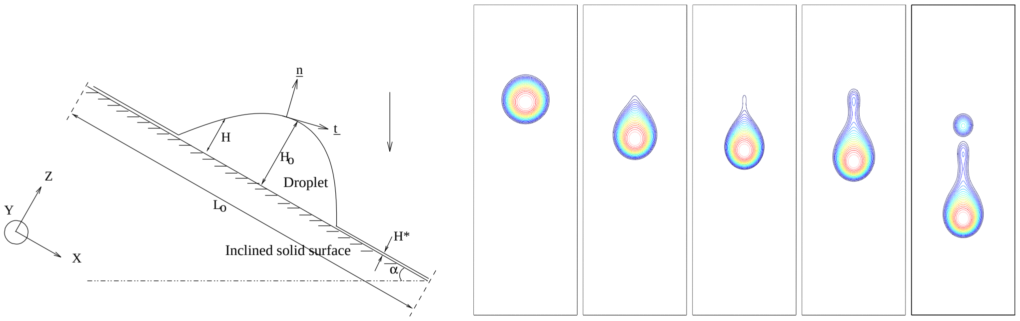

(a) (b) (c) (d) (e) (f)

Fig. 1. (a) Schematic of droplet motion down an inclined plane; computed contour plots showing different modes of droplet migration with varying inclination angle, α: (b) 20^o ($U = 0.2$m/s), (c) 35^o ($U = 0.27$m/s), (d) 40^o ($U = 0.03$m/s), (e) 45^o ($U = 0.036$m/s) and (f) 60^o ($U = 0.048$m/s).

grids ($O(10^5)$ grid points), a recent study by Koh [10] has shown that far greater grid densities are required to obtain grid- and precursor film thickness-independent solutions even for simple droplet motions.

This paper combines recent advances in the development of highly efficient Multigrid methods [4] for solving the associated lubrication equations used to model droplet migration with the implementation of parallel computing architectures to present a quantitative comparison of droplet migration speeds with those measured in the recent experiments of Podgorski et al [8] and LeGrand et al [9].

2 Problem Description

The problem considered is illustrated schematically in Fig. 1(a) showing the motion of a droplet migrating down an inclined plane. Assuming that the ratio, $\epsilon = H_0/L_0$, relating the characteristic droplet thickness to the extent of the substrate, is small, the Navier-Stokes equations reduce to the simpler, non-dimensional lubrication equations of the form:

$$\frac{\partial h}{\partial t} = \frac{\partial}{\partial x}\left[\frac{h^3}{3}\left(\frac{\partial p}{\partial x} - \frac{Bo}{\epsilon}\sin\alpha\right)\right] + \frac{\partial}{\partial y}\left[\frac{h^3}{3}\left(\frac{\partial p}{\partial y}\right)\right] \ , \tag{1}$$

$$p = -\nabla^2(h) - \mathit{\Pi}(h) + Bo\cos\alpha(h) \ , \tag{2}$$

where h and p are the non-dimensional dependent variables for film thickness and pressure, α is the substrate inclination angle, and, $Bo = \rho g L_0^2/\sigma$, is the Bond number. The disjoining pressure term is:

$$\mathit{\Pi}(h) = \frac{(n-1)(m-1)(1-\cos\theta_s)}{h^*(n-m)\epsilon^2}\left[\left(\frac{h^*}{h}\right)^n - \left(\frac{h^*}{h}\right)^m\right] \ , \tag{3}$$

where θ_s is the equilibrium static contact angle, σ is surface tension; constants n and m are the exponents of the interaction potential, chosen to be 3 and 2, respectively. Further details can be found in [4].

A contact angle hysteresis model is built in, based on the droplet motion history; in which static advancing and receding contact angles, $\theta_{s,a}$ and $\theta_{s,r}$, are assigned to equation (3), depending on the motion of the droplet [10].

3 Method of Solution

Following [4], a system of differential-algebraic equations is obtained by application of finite-difference discretisation on a quadrilateral mesh with equal spacings in the x and y directions.

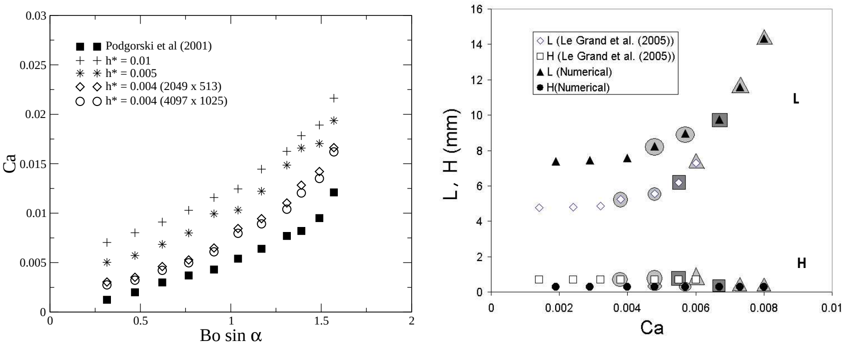

(a) (b)

Fig. 2. Quantitative comparison between experimental data and numerical predictions of droplet migration on an inclined plane: (a) Podgorski et al [8]; (b) LeGrand et al [9]. The plot in (a) shows the accuracy of the numerical solution improves with smaller pre-cursor film thickness, h^*, and (b) delineates the change in droplet shape with varying droplet speed.

Time integration is performed using an implicit, second-order scheme with adaptive step-size selection based upon a local truncation error estimate. At each time step, the nonlinear discretized equations are solved using a full approximation storage and full Multigrid scheme (FAS-FMG)[11]. Parallel implementation of the solver is achieved via a geometric decomposition of the computational domain, based on a partitioning strategy of the coarsest grid used. Its basic philosophy follows that employed in [12] and is described in greater detail in [10].

4 Results and Discussion

The data from two experimental studies investigating the effects of inclination angle, α, on droplet shape and wetting speed is compared with corresponding results obtained using the lubrication-based parallel Multigrid solver. The first case considers data obtained by Podgorski et al [8] where a silicon oil droplet of radius 1mm and volume 8.3mm^3 with $\rho = 924$ kg/m^3, $\mu = 0.00915$ Pas and $\sigma = 0.0205$ N/m at 25^oC, is used (see Fig. 1). Their reported static advancing and receding contact angles, $\theta_{s,a} = 50^o$, and, $\theta_{s,r} = 40^o$, respectively were employed in the simulations. The latter were performed on a rectangular domain (385 × 129 grid points; $H^* = 26\mu$m) and predictions of the effects of varying inclination angle, α, on droplet shape with $L_o = 4$ mm, are seen to be in excellent agreement with the data of Podgorski et al [8]. They display smooth rounded contact lines and angled corner shaped tails at low velocities, and cusp formation and pearling at the higher velocities induced at high inclination angles.

Of even greater interest is the effect of α on steady droplet speed, data for which is given in the form of a Capillary number ($Ca = \mu U/\sigma$) versus $Bo \sin\alpha$ graph; Fig. 2(a) shows that there is a strong dependence of the over-prediction of droplet speed on the value of h^*. With $h^* = 0.01$ (corresponding to $H^* = 26\mu$m), speeds are over-predicted by a factor between 6 and 2. A 60% reduction in h^* to 0.004 ($H^* = 10.4\mu$m) leads to a significant improvement; with predicted values being reduced to a factor between 2 and 1.34, respectively. The effect of grid density on solution accuracy is shown more clearly in the left half of Table 1. As expected, significantly larger computational resources are required to obtain grid-independent solutions; for the latter case, over 4 million grid points are needed. Even greater resources are required for h^* values nearer the physically realistic range [10].

The experiments of LeGrand et al [9], consider the motion of a 6 mm^3 oil droplet of radius 2 mm with $\rho = 936$ kg/m^3, $\mu = 0.01$ Pas and $\sigma = 0.0201$ N/m on a surface with $\theta_{s,a} = 51^o$ and $\theta_{s,r} = 46^o$. Sample simulations were performed with $h^* = 0.005$ ($H^* = 2.4\mu$m) and $L_o = 8$ mm, on a rectangular domain with over 1 million grid points. The right half of Table 1 provides a comparison between the experimentally and numerically obtained values of Ca as a function

$Bo\sin\alpha$	$Ca_{(Pod)}$	Ca_{grid1}	$\frac{Ca_{grid1}}{Ca_{(Pod)}}$	Ca_{grid2}	$\frac{Ca_{grid2}}{Ca_{(Pod)}}$	$Bo\sin\alpha$	$Ca_{(LeG)}$	Ca_{grid1}	$\frac{Ca_{grid1}}{Ca_{(LeG)}}$
0.32	0.0012	0.0030	2.45	0.0028	2.21	0.39	0.0014	0.0019	1.36
0.47	0.0020	0.0035	1.76	0.0032	1.61	0.52	0.0024	0.0029	1.21
0.62	0.0030	0.0046	1.53	0.0042	1.41	0.64	0.0032	0.0040	1.25
0.91	0.0043	0.0065	1.50	0.0061	1.42	0.75	0.0038	0.0048	1.26
1.04	0.0054	0.0084	1.56	0.0080	1.47	0.86	0.0048	0.0057	1.20
1.31	0.0077	0.0110	1.43	0.0104	1.35	0.97	0.0055	0.0067	1.21
1.49	0.0095	0.0142	1.49	0.0135	1.42	1.06	0.0060	0.0073	1.21
1.57	0.0121	0.0166	1.49	0.0162	1.34	1.16	0.0065	0.0080	1.23

Table 1. Comparison between experimental and predicted Ca values as a function of $Bo\sin\alpha$. (Left) Data of Podgorski et al [8], $Ca_{(Pod)}$, and (Right) of LeGrand et al [9], $Ca_{(LeG)}$. Grid 1 has 2049 × 513 uniformly spaced grid points and grid 2 has 4097 × 1025 points.

of $Bo\sin\alpha$. The quantitative agreement between the two is very good, where speeds are being predicted to within 20% of many of the experimental values.

Le Grand et al [9] also measured the length, L, and maximum height, H, of the droplet as a function of Ca. A comparison between their experimental results and numerical prediction is given in Fig. 2(b). They show that, H, remains effectively constant as L increases at higher α. The predicted lengths, L, are typically 50% larger than those reported in experiments at small Ca, whereas the agreement between the predicted heights, H, is consistently good. The shapes of the droplets that result are also indicated in Fig. 2(b), where data without any shading indicates that the droplets are rounded, as shown in Fig. 1(b), whereas rounded shading, square shading and triangular shading represents droplet shapes with corner (Fig. 1(c)), cusp (Fig. 1(d) and 1(e)) and pearling (Fig. 1(f)) characteristics. The data shows that corner to cusp to pearling transitions as observed experimentally, occurs at smaller droplet speeds than predicted numerically. Finally, note that the cusp angle at which pearling transition occurs has also been considered numerically by Koh [10], who obtained good agreement with the experiments reported in [9].

5 Conclusion

Although lubrication theory displays good qualitative agreement with experimental observation of droplet migration when relatively coarse grids are used to solve the model equations, both precursor film thickness, h^*, and grid density have an important influence on the predicted accuracy of key features such as droplet speed. In that, much finer grids are required together with small precursor film thicknesses to obtain grid independent solutions commensurate with experiment.

References

1. T.D. Blake, K.J. Ruschak, *Liquid Film Coating* (Chapman and Hall, 1997), 63-97.
2. A. Oron, S. Davis, S. Bankoff, Rev. Mod. Phys. **69**, (1997) 931.
3. L.W. Schwartz, R.R. Eley, J. Colloid Interface Science **202**, (1998) 173-188.
4. P.H. Gaskell, P.K. Jimack, M. Sellier, H.M. Thompson, Int. J. Num. Meth. Fluids **45**, (2004) 1161-1186.
5. L.W. Schwartz, D. Roux, J.J. Cooper-White, Physica D **209**, (2005) 236-244.
6. L.W. Schwartz, R.V. Roy, R.R. Eley, H.M. Princen, J. Eng. Math. **50**, (2004) 157-175.
7. A.L. Bertozzi. Notices of the AMS. **45(6)**, (1998), 689-697.
8. T. Podgorski, J. Flesselles, L. Limat, Phys. Rev. Lett. **87**, (2001) 036102(1).
9. N. LeGrand, A. Daerr, L. Limat, J. Fluid Mech. **541**, (2005) 293-315.
10. Y.Y. Koh, PhD thesis, University of Leeds, 2007.
11. Y.C. Lee, H.M. Thompson, P.H. Gaskell, Comp. Fluids **36**, (2007) 838-855.
12. C.E. Goodyer, M. Berzins, Concurrency and Computation **19**, (2007) 369-396.